HHS Public Access

Author manuscript

J Immunol. Author manuscript; available in PMC 2018 November 15.

Published in final edited form as:

J Immunol. 2017 November 15; 199(10): 3525–3534. doi:10.4049/jimmunol.1701011.

Genetic control of Lyme arthritis by *Borrelia burgdorferi* arthritis-associated locus 1 (*Bbaa1*) is dependent on localized differential production of IFN-β and requires upregulation of myostatin

Jackie K. Paquette[*], **Ying Ma**[*], **Colleen Fisher**[*], **Jinze Li**[*], **Sang Beum Lee**[†], **James F. Zachary**[‡], **Yong Soo Kim**[†], **Cory Teuscher**[§], and **Janis J. Weis**[*]

[*]Department of Pathology, University of Utah, Salt Lake City, Utah, USA

[†]Department of Human Nutrition, Food, and Animal Sciences, University of Hawaii at Mānoa, Honolulu, Hawaii, USA

[‡]Department of Veterinary Pathobiology, University of Illinois at Urbana-Champaign, Urbana, Illinois, USA

[§]Department of Medicine, University of Vermont, Burlington, Vermont, USA

Abstract

Previously, using a forward genetic approach we identified differential expression of type I IFN as a positional candidate for an expression quantitative trait locus (eQTL) underlying *B. burgdorferi* arthritis-associated locus 1 (*Bbaa1*). In this study, we show that mAb blockade revealed a unique role for IFN-β in Lyme arthritis development in B6.C3-*Bbaa1* mice. Genetic control of IFN-β expression was also identified in bone marrow-derived macrophages stimulated with *B. burgdorferi,* and was responsible for feed-forward amplification of interferon-stimulated genes. Reciprocal radiation chimeras between B6.C3-*Bbaa1* and B6 mice revealed that arthritis is initiated by radiation-sensitive cells, but orchestrated by radiation-resistant components of joint tissue. Advanced congenic lines were developed to reduce the physical size of the *Bbaa1* interval, and confirmed the contribution of type I IFN genes to Lyme arthritis. RNA-seq of resident $CD45^{-}$ joint cells from advanced interval specific recombinant congenic lines identified myostatin as uniquely upregulated in association with *Bbaa1* arthritis development, and myostatin expression was linked to IFN-β production. Inhibition of myostatin *in vivo* suppressed Lyme arthritis in the reduced interval *Bbaa1* congenic mice, formally implicating myostatin as a novel downstream mediator of joint-specific inflammatory response to *B. burgdorferi*.

Corresponding author: Janis J. Weis, 15 North Medical Drive East, Salt Lake City, Utah 84112-5650, USA. Phone: 801.585.2417; janis.weis@path.utah.edu.

Data deposit

The RNA-seq data presented in this article have been submitted to the National Center for Biotechnology Information Gene Expression Omnibus repository (https://www.ncbi.nlm.nih.gov/geo/) under accession number GSE102748.

Disclosures: The authors have declared that no conflict of interest exists.

Introduction

Lyme disease, caused by infection with the bacteria *Borrelia burgdorferi*, affects 300,000 Americans each year (1). Disease outcomes range from acute to chronic, sometimes resulting in irreversible damage to the nervous (2) and cardiovascular (3, 4) systems. Arthritis is the most common late disease manifestation (5), affecting up to 60% of patients and persisting in 10% of patients despite antibiotic therapy (6). Lyme arthritis is frequently characterized by synovitis at one or both knee joints and may persist for years after infection (6, 7). While both bacterial and host factors contribute to the spectrum of Lyme disease severity (8), many studies have shown that severe Lyme arthritis can result from genetically controlled dysregulated immune responses (9–17).

The spectrum of disease severity in humans can be modeled in inbred strains of mice, which display different disease outcomes upon infection with *B. burgdorferi* (13). Specifically, C57BL/6 (B6) mice develop mild arthritis and C3H mice develop severe arthritis in response to the same *B. burgdorferi* inoculum. We have successfully employed these mice during empirical (18–20) and forward genetic (21–23) approaches to identify genetic determinants of Lyme arthritis severity. Empirical approaches comparing the global gene expression profiles of B6 and C3H joint tissue revealed a type I IFN signature in C3H mice that is absent from B6 mice (18), and a receptor-blocking antibody and receptor ablation showed that type I IFN is required for maximally severe Lyme arthritis (19, 20). Independently, forward genetic approaches identified a quantitative trait locus, *Bbaa1*, that contains the type I IFN gene cluster and controls Lyme arthritis severity (21). An interval specific congenic line in which the $Bbaa1^{C3H}$ allele was introgressed onto the B6 background (B6.C3-*Bbaa1*) displays increased Lyme arthritis relative to B6 mice (21) unless pretreated with the type I IFN receptor-blocking antibody (22), functionally linking the expression of type I IFN within *Bbaa1* to increased Lyme arthritis. Interestingly, $Bbaa1^{C3H}$ was also found to control disease severity in the K/B’N serum transfer model of rheumatoid arthritis (RA) through type I IFN production (22), indicating that insight gleaned from our model extends to a distinct inflammatory arthritis.

Our finding of a pathologic type I IFN profile is consistent with several publications that have shown a type I IFN signature in the serum of human Lyme patients at stages of active disease (2, 24) and in the synovial fluid of treatment-refractory RA patients (25). Arthritis is also a transient side effect in hepatitis C and multiple sclerosis patients treated with IFN-α/β (26, 27), further supporting the linkage between elevated levels of type I IFN and arthritis. However, type I IFN is a key element in the innate and adaptive response against a variety of microbial infections, posing an inherent problem to treatment blockade. Because type I IFN regulation requires a sensitive balance, and because IFN-α and IFN-β members play unique roles in various infections, we sought to identify the specific type I IFN and downstream mediators Lyme arthritis pathogenesis. Herein, the B6.C3-*Bbaa1* mouse allowed us to identify the specific type I IFN member that causes *Bbaa1* Lyme arthritis, segregate cells that initiate type I IFN in *B. burgdorferi* infection from those that respond to it, and illuminated myostatin as an unexpected mediator of IFN-regulated Lyme arthritis development.

Materials and Methods

Mice

B6 and C3H mice were obtained from Jackson Laboratories. B6.C3-*Bbaa1* mice (Chr4: 11.6–93.46 Mbp) were previously generated (21) and maintained as a colony in our Animal Research Center (Salt Lake City, UT). Interval specific recombinant congenic lines (ISRCL1-4) with Chr4 *Bbaa1* intervals 11.6–77.8 Mbp, 76.48–93.46 Mbp, 83.7–93.46 Mbp, and 88.3–93.46 Mbp were independently generated through repeated backcrosses of B6.C3-*Bbaa1* to the parental B6 line. Filial offspring were selected based on SNP identification by high-resolution melting analysis as described (28), and homozygous lines were fixed by mating littermates. All mice used in this study were housed in the University of Utah Animal Research Center (Salt Lake City, UT) and handled with protocols approved by the Institutional Animal Care and Use Committee at the University of Utah in accordance with the NIH guidelines for the care and use of animals.

B. burgdorferi cultures, infections, and arthritis assessments

B. burgdorferi strain N40 was cultured for 4 days in Barbour-Stoenner-Kelly II (BSK) medium containing 6% rabbit serum (Sigma-Aldrich). Mice were infected with 2×10^4 live spirochetes intradermally into the skin of the back (29). Arthritis was assessed by rear ankle joint measurements obtained with a metric caliper at days 0 and 28 post infection, and by histopathological analysis of the most severely swollen rear ankle joint following fixation, decalcification, and H&E staining as described previously (30). Histopathological scores were determined blindly and ranged from 0 to 5 for various aspects of disease, including severity and extent of the lesion, PMN leukocyte and mononuclear cell (e.g. monocyte, macrophage) infiltration, tendon sheath thickening (e.g. synoviocyte and fibroblast hypertrophy/hyperplasia), and reactive/reparative responses (e.g. periosteal hyperplasia and new bone formation and remodeling), with 5 representing the most severe lesion and 0 representing no lesion. Infection was confirmed in mice euthanized 28 days post infection by ELISA quantification of *B. burgdorferi* specific IgG concentrations in serum (31) and *16S rRNA B. burgdorferi* transcripts in joints (18, 32) or *B. burgdorferi* DNA in ear tissue (33).

Inhibitory reagents and treatments

Monoclonal Abs were used to neutralize murine IFNAR1 (MAR1-5A3), IFN-α (TIF-3C5), or IFN-β (HDβ-4A7) (Leinco Technologies, Inc.). TIF-3C5 is considered a “pan-IFN-α” mAb because it neutralized all IFN-α subtypes available for testing: αA, α1, α4, α5, α11, and α13 (34). Mice received mAbs or isotype controls by intraperitoneal injection following a dosage regimen described previously (34, 35). Briefly, anti-IFNAR1 was administered in a single 2.5 mg dose the day before infection with *B. burgdorferi* (19, 22, 35), anti-IFN-β was administered in two doses (300 μg each, 600 μg total) the day before and 2 days following infection, and anti-IFN-α was administered in three doses (333 μg each, 1 mg total) the day before and days 1 and 3 post infection. Boosts were determined based on pharmacokinetics previously reported (34) and in consideration with the IFN profile peak 7 days post infection with *B. burgdorferi* (18). For BMDM experiments, 10 μg/ml of each mAb was administered in combination with the stimulation. The myostatin inhibitor (MBP-fMSTNpro45-100-Fc) is a recombinant peptide containing C-terminal mouse Fc domain fusion to the fish truncated

propeptide-1, the production of which was described previously (36). The Fc fusion did not affect myostatin-inhibitory activity of the truncated propeptide-1, with the potency comparable to commercial full-length mammalian myostatin propeptide (Supplemental Fig. 4). Mice received four intraperitoneal injections of vehicle (PBS) or myostatin inhibitor (400 μg each, 1.6 mg total) once weekly beginning the day after infection.

Generation of reciprocal radiation chimeras

Chimeras were generated in all pairwise combinations between B6 (CD45.1), B6 (CD45.2), and B6.C3-*Bbaa1* (CD45.2) using a rapid reconstitution protocol as described (20, 37). Rapid reconstitution involves transplanting donor splenocytes into irradiated recipient mice and allows for the infection of young mice <8 wk old, necessary for a reliable arthritis phenotype. Chimerism was evaluated by flow cytometric analysis of peripheral blood leukocytes 25 days post transplant (Supplemental Fig. 2A).

Isolation of CD45$^-$ cells from joint tissue

Mouse rear ankle joints were gently digested into single-cell suspensions as described (20). Briefly, skin was removed and tibiotarsal tissue was teased away from bone using 20-gauge syringe needles followed by 1 h incubation at 37°C in RPMI 1640 containing 0.2 mg/ml endotoxin-free Liberase TM (Roche) and 100 μg/ml DNase I (Sigma-Aldrich). Single-cell suspensions were filtered through a 100 μm cell strainer, RBCs were lysed in ammonium-chloride-potassium buffer, and cells were labeled with biotinylated anti-CD45.2 (BioLegend) followed by streptavidin magnetic bead labeling (Miltenyi Biotec). Magnetic bead separation was performed on MS columns (Miltenyi Biotec) according to the manufacturer's instructions. Flow cytometric analysis revealed >85% purity in the CD45$^-$ fraction, as previously reported (20). CD45$^-$ cells from both rear ankle joints of two mice were pooled for each *n* sample in order to increase RNA concentration for transcript analysis (Fig. 6, 7A). For *ex vivo* stimulation, CD45$^-$ cells from both rear ankle joints of >8 mice were pooled, plated in RPMI 1640 containing 2% FBS (20), and stimulated with live *B. burgdorferi* (6×10^6/ml) or 100 U/ml IFN-β (PBL Laboratories) for 3 h (Fig. 7B, Supplemental Fig. 3).

Cell culture

BMDMs were prepared by culturing bone marrow isolated from the femurs and tibias of mice for 7 d in L929 cell-conditioned media as a source of M-CSF, as previously described (38). Harvested macrophages were then replated in 24-well dishes at a density of 6×10^5/ml in media containing 1% of the serum replacement Nutridoma (Roche). Cultures were stimulated with live *B. burgdorferi* (6×10^6/ml) for 6 h at 37°C with 5% CO_2.

Flow cytometric analysis of P-Stat 1

Phosphorylated Stat1 was stained as described (34, 39) following 15 h incubation with *B. burgdorferi* and type I IFN blocking mAbs. Briefly, cells were incubated in 0.05% trypsin (Fisher Scientific) and scraped to detach from plate. Cells were fixed using 1.5% paraformaldehyde and permeabilized with 100% methanol. P-Stat1 was stained using an unconjugated Phospho-Stat1 mAb (pY701, Cell Signaling) at a 1:200 dilution and incubated

for 1 h at RT, followed by a secondary stain with Goat anti-Rabbit IgG conjugated to Alexa Fluor 647 (Fisher Scientific) at a 1:500 dilution and incubated for 30 min at RT. Data were collected on a FACSCanto II (BD Biosciences) flow cytometer and analyzed using FlowJo v. 10.0.8 software.

Gene expression analysis

Total RNA was recovered using TRIzol reagent (Invitrogen) and purified using the Direct-zol RNA MiniPrep kit (Zymo Research). For RNA-sequencing, libraries were prepared using PolyA enrichment and sequenced with Illumina HiSeq 50 Cycle Single-Read Sequencing version 4 at the University of Utah High Throughput Genomics Core Facility (Salt Lake City, UT). Sequences were annotated with help from the University of Utah Bioinformatics Core Facility (Salt Lake City, UT). Briefly, reads were aligned to the mouse genome from Ensembl release 87 using STAR (40) and assigned to genes using featureCounts (41). Differentially expressed genes were identified using a 5% false discovery rate with DESeq2 (42). The RNA-seq data presented in this article have been deposited in the National Center for Biotechnology Information Gene Expression Omnibus repository (https://www.ncbi.nlm.nih.gov/geo/), with the accession number GSE102748. For qRT-PCR analyses, RNA was reverse transcribed, and transcripts were quantified using a Roche LC-480 according to our previously described protocols (21). Primer sequences used in this study for *β-actin, Iigp* (18), *Oasl2, Cxcl10, Tyki* (19), *Gbp2* (43), *Tnfa,* and *Ifnb* (44) can be found at the indicated citations. *Mstn* primer sequences designed in this study were as follows: forward (5′-GATCTTGCTGTAACCTTCCC-3′) and reverse (5′-CTCCTGAGCAGTAATTGGC-3′).

Data and statistical analyses

All graphical data depict the mean ± SEM. Statistical calculations were performed using GraphPad Prism 7.0b software. Continuous variables were analyzed by one-way ANOVA with Dunnett's post hoc test for pairwise comparisons or Student's *t* test (2-tailed). Categorical variables were analyzed by the Mann-Whitney *U* test (2-tailed). Statistical significance (*$p < 0.05$, **$p < 0.01$, ***$p < 0.001$, ****$p < 0.0001$) is indicated.

Results

Determination of the proarthritogenic type I IFN cytokine in B6.C3-*Bbaa1* mice

Both empirical and forward genetic studies from our lab have converged on the finding that a pathologic type I IFN profile drives Lyme arthritis in C3H mice (18–22). In this regard, we identified differential expression of type I IFN as a positional candidate for an expression quantitative trait locus (eQTL) underlying *B. burgdorferi* arthritis-associated locus 1 (*Bbaa1*) (22). Nevertheless, there are multiple members of the type I IFN family, with the IFN-α and IFN-β subclasses playing the largest roles in pathogenesis to date, and although each signals through a shared receptor heterodimer, their unique roles in host protection and pathogenesis are becoming increasingly appreciated (34, 45).

To assess the specific contribution of IFN-α and IFN-β to Lyme arthritis development, B6.C3-*Bbaa1* mice were treated with a pan-acting mAb that blocks multiple IFN-α subtypes

(TIF-3C5) or a mAb that targets IFN-β specifically (HDβ-4A7). We previously showed that the anti-IFNAR1 mAb (MAR1-5A3) suppresses arthritis development to the baseline of B6 (22). Because blocking IFN-β resulted in the same reduction in Lyme arthritis as blocking IFNAR1 (Fig. 1A), we conclude that IFN-β and not IFN-α is the proarthritic cytokine generated in B6.C3-*Bbaa1* mice. Analysis of anti-*B. burgdorferi* IgG in the serum and *B. burgdorferi 16S rRNA* transcripts in the joint confirm that blocking type I IFN does not impact the ability of the host to generate a B-cell response or to control infection (Fig. 1B). Taken together, these findings suggest that differential expression of IFN-β, and not IFN-α, may be the eQTL within *Bbaa1* controlling the severity of Lyme arthritis.

Effect of blocking IFN-α or IFN-β on type I IFN activation in BMDMs

We previously showed that bone marrow-derived macrophages (BMDMs) from B6.C3-*Bbaa1* mice express higher levels of IFN-inducible transcripts in response to *B. burgdorferi* than do BMDMs from B6 mice (22). Thus, B6.C3-*Bbaa1* BMDMs were used as a surrogate for myeloid cells in joint tissue to assess the specific contribution IFN-α or IFN-β to the *Bbaa1*-directed induction of type I IFN. BMDMs were stimulated with *B. burgdorferi* and simultaneously treated with each mAb for 6 h. Isotype control mAbs had no effect, as shown for murine IgG_{2a} (Supplemental Fig. 1A). Treatment with anti-IFN-β resulted in complete suppression of IFN-inducible genes, indistinguishable from levels of macrophages treated with IFN receptor blockade (Fig. 2A). In contrast, treatment with anti-IFN-α had no effect on the expression of IFN-inducible genes, indicating that IFN-β is the critical eQTL within *Bbaa1* driving Lyme arthritis development. Importantly, none of these treatments impacted the expression of *Tnfa* (Fig. 2A), which is downstream of the critical MyD88-dependent host defense pathway (46, 47). This highlights the *in vivo* observation that type I IFN is not required for host defense in Lyme arthritis (Fig. 1B), and its suppression does not influence the expression of initial MyD88-dependent cytokines (20, 22)

Because Stat1 is phosphorylated when IFN-α and IFN-β proteins bind the receptor (34, 48), flow cytometric analysis of phosphorylated Stat1 protein was used as a complementary approach to determine the impact of IFN-α and IFN-β on feed-forward IFN amplification. In order to allow for transcription and translation of type I IFN proteins, Stat1 phosphorylation was assessed in BMDMs 15 h post stimulation with *B. burgdorferi* and mAb treatment. Strikingly, IFN-β neutralization completely inhibited Stat1 phosphorylation, similar to levels in macrophages treated with receptor blocking mAb, while blocking IFN-α had no effect (Fig. 2B). Because anti-IFN-α did not impact arthritis severity or macrophage responses to *B. burgdorferi,* mAb functionality was assessed with recombinant IFN-α (Supplemental Fig. 1B). Confirmation of anti-IFN-α activity supports the conclusion that IFN-β (but not IFN-α) is the type I IFN made in response to *B. burgdorferi* both *in vivo* and *in vitro,* and that not even low levels of IFN-α contribute to the feed-forward response. Interestingly, Stat1 deficiency was previously reported not to influence arthritis severity in *B. burgdorferi* infected C3H mice (49), suggesting that the macrophage responses of congenic mice may allow a focused appreciation of Stat1 involvement in type I IFN signaling that may be limited by the activation of compensatory pathways in the joint tissue.

Does *Bbaa1* initiate arthritis through hematopoietic or resident cells?

Multiple lines of evidence indicate that differential expression of IFN-β may be the eQTL underlying *Bbaa1*, leading to the question of whether the proarthritic effect of IFN-β expression acts through hematopoietic or resident cells. MHC compatibility between mildly arthritic B6 mice and more severely arthritic B6.C3-*Bbaa1* mice allowed reciprocal radiation chimeras to be generated (Fig. 3A). Using a rapid reconstitution protocol previously developed by our laboratory (see Materials & Methods), myeloid compartments were sufficiently reconstituted by donor-derived cells (~80%) prior to infection (Supplemental Fig. 2A), and reconstitution was determined to be adequate for host defense based on the similar abilities of irradiated mice to control infection (Supplemental Fig. 2B).

As expected, B6 mice reconstituted with autologous splenocytes (B6→B6) developed mild arthritis and B6.C3-*Bbaa1* mice reconstituted with autologous splenocytes (*Bbaa1*→*Bbaa1*) developed more severe arthritis 4 wk post infection with *B. burgdorferi* (Fig. 3B). Notably, B6.C3-*Bbaa1* mice reconstituted with hematopoietic cells from B6 mice (B6→*Bbaa1*) displayed mild arthritis compared to *Bbaa1*→*Bbaa1* chimeras, and B6 mice reconstituted with cells from B6.C3-*Bbaa1* mice (*Bbaa1*→B6) developed greater arthritis than B6→B6 (Fig. 3B). Thus, genes encoded within *Bbaa1* regulate Lyme arthritis severity through the radiosensitive, hematopoietic cellular constituents of the joint.

Considering that differential expression of IFN-β may be the eQTL underlying *Bbaa1*, we can further deduce that radiosensitive cells in the joint, which are likely myeloid (20), initiate the production of proarthritic IFN-β (Fig. 3C). This is consistent with our previous findings that $CD45^+$ cells harvested from a naïve mouse joint possess the unique ability to generate an IFN profile upon *ex vivo* stimulation with *B. burgdorferi,* whereas $CD45^-$ cells are capable of responding to but not initiating type I IFN in response to *B. burgdorferi* (Supplemental Fig. 3 and ref. 20). Another striking finding is that *Bbaa1*→B6 chimeras develop the full arthritis phenotype, strongly implicating that regardless of genotype, radioresistant-resident cells are fully competent to choreograph arthritis manifestation in the joint (Fig. 3B, 3C). This is consistent with the previous finding that endothelial cells and fibroblasts, both of which are radioresistant cell types in the joint, are major responders to and amplifiers of type I IFN, resulting in production of chemokines in infected C3H mice (20). This provides the first *in vivo* evidence for the “pass off” that occurs between cells that initiate IFN-β in response to *B. burgdorferi* and cells that respond to IFN-β to direct arthritis development (Fig. 3C).

C3H-derived *Bbaa1* genes spanning the type I IFN locus confer increased arthritis on B6 background

Because the original B6.C3-*Bbaa1* congenic interval was very large (Chr4: 11.6–93.46 Mbp) with >450 genes in addition to *Ifnb*, we generated and studied a panel of overlapping interval specific recombinant congenic lines across *Bbaa1* (ISRCL1-4). This allowed us to further interrogate the relationship between differential expressions of IFN-β as an eQTL for *Bbaa1* and the pathogenesis of Lyme arthritis (Fig. 4). ISRCL1 encompasses the largest portion of the $Bbaa1^{C3H}$ interval but excludes the type I IFN locus, while ISRCL2-4 retain the C3H type I IFN gene cluster with further reduction in the amount of C3H donor

sequence (Fig. 4). Phenotypic analysis following infection with *B. burgdorferi* revealed that arthritis severity co-segregates with the C3H derived type I IFN locus (Fig. 4). Because blocking IFN-β in the B6.C3-*Bbaa1* mice completely suppressed Lyme arthritis (Fig. 1A), we deduce that the phenotype in ISRCL2-4 mice is similarly dependent on IFN-β production.

BMDMs were used to confirm that genes contributing to heightened IFN-β expression are retained in the narrowed *Bbaa1* interval. Macrophages from ISRCL3 and ISRCL4 mice, which both possess the C3H allele for the type I IFN locus, displayed greater IFN-inducible transcriptional responses for *Cxcl10* and *Gbp2* than macrophages from B6 mice, with trending differences for other transcripts (Fig. 5). However, macrophages from the congenic mice failed to attain the maximal level of IFN signature transcripts seen in macrophages from C3H mice, indicating additional genetic loci contribute to the fully expressed IFN response in C3H mice. As shown, *Ifnb* expression is low, but none of the IFN-α transcripts were detectable, further supporting the role of IFN-β in driving Lyme arthritis pathogenesis. The narrowed *Bbaa1* congenic lines, ISRCL3 & ISRCL4, have provided a refined tool to study the involvement of type I IFN in Lyme arthritis.

How do expression polymorphisms within *Bbaa1* change the transcriptome of the radioresistant-resident responders?

Now that we have established the role of radioresistant-resident cells in directing *Bbaa1* Lyme arthritis downstream of IFN-β, we pursued a better understanding of the mechanism of arthritis development through transcriptome analysis of $CD45^-$ (resident) joint cells. Newly developed ISRCL3 and ISRCL4 lines were compared to B6 mice in order to capture all genes related to IFN-β production and arthritis development with a minimal physical interval. To capture the stage of active arthritis development (as opposed to full-blown arthritis with confounding wound repair pathways), joint cells were harvested from mice 22 days post infection with *B. burgdorferi* (29). Following recovery of single-cell suspensions, the $CD45^-$ population was isolated by magnetic bead separation and RNA-seq was performed.

Not surprisingly, comparing the transcriptomes of these highly similar genotypes at a time point submaximal to arthritis development revealed very few differences in gene expression profiles (Fig. 6A). Of those differences, only five genes were independently identified in both ISRCL4 vs. B6 and ISRCL3 vs. B6 comparisons with ≥ 1.5-fold change (in either direction) and p-adj <0.05 (Fig. 6A, Table I), supporting their involvement in *Bbaa1*-directed Lyme arthritis. Importantly, myostatin (*Mstn*) had the greatest induction and achieved the highest level of significance in independent analyses with both interval specific congenic lines (Fig. 6A, Table I), illuminating it as a strong candidate for *Bbaa1* Lyme arthritis development. Quantitative RT-PCR analysis of *Mstn* expression in $CD45^-$ cells from uninfected animals revealed similar expression among uninfected mice of all three genotypes (data not shown), and revealed that genes within *Bbaa1* specifically regulate the induction of myostatin following infection with *B. burgdorferi* (Fig. 6B). This was a striking finding for *Bbaa1* Lyme arthritis development in light of recent evidence that myostatin is involved in RA development in humans and mice (50).

Impact of IFN-β on myostatin expression in CD45⁻ cells isolated from joint tissue

To ascertain a direct effect between IFN-β production and myostatin expression in *Bbaa1* Lyme arthritis, IFN-β was blocked in ISRCL4 and ISRCL3 mice infected with *B. burgdorferi* (as described in Fig. 1). CD45⁻ cells were isolated from joint tissue 22 days post infection, and myostatin expression was assessed by qRT-PCR. Importantly, CD45⁻ cells from ISRCL4 and ISRCL3 mice infected with *B. burgdorferi* and treated with anti-IFN-β mAb displayed a 2-fold reduction in *Mstn* transcripts compared to mice treated with isotype control (Fig. 7A). The fold suppression by blocking IFN-β is internally consistent with the level of induction found in our RNA-seq (Fig. 6). This directly connects the genetic control of differential expression of IFN-β to the regulation of myostatin expression as a downstream effector.

Several proinflammatory cytokines, TNF-α, IL-1α, and IL-17, were previously shown to directly induce expression of myostatin in the context of RA, but the impact of IFN-β was not addressed (50). To test whether IFN-β directly induces expression of myostatin, CD45⁻ cells were isolated from the joints of naïve B6 mice and stimulated *ex vivo* with IFN-β, *B. burgdorferi,* or IFN-β and *B. burgdorferi* in combination. *Mstn* expression assessed by qRT-PCR revealed that IFN-β works synergistically with *B. burgdorferi* to directly induce *Mstn* expression (Fig. 7B). To our knowledge, this is the first report of IFN-β induction of myostatin.

Inhibition of myostatin suppresses Lyme arthritis in *Bbaa1* congenic mice

In order to determine whether myostatin is a marker or a mediator of *Bbaa1* Lyme arthritis, infected ISRCL4 and ISRCL3 mice were treated with an inhibitory propeptide of myostatin, known to efficiently bind myostatin and block it from interacting with its receptors both *in vivo* and *in vitro* (Supplemental Fig. 4 and ref. 36, 50), and the impact on arthritis development was assessed. Consistent with the dual requirement of *B. burgdorferi* and IFN-β for myostatin upregulation (Fig. 7A, 7B), myostatin inhibition did not impact ankle swelling in uninfected animals (Fig. 8A). However, myostatin inhibition in infected ISRCL4 and ISRCL3 mice led to a remarkable suppression in arthritis 4 wk post infection with *B. burgdorferi* (Fig. 8A, 8B). Importantly, myostatin inhibition did not impact host defense, as anti-*B. burgdorferi* IgG in the serum and *B. burgdorferi* numbers in tissues were similar between treated and untreated groups (Fig. 8C). These findings demonstrate a direct effect of myostatin on joint-specific inflammatory responses.

Discussion

In this study, we established IFN-β as the Lyme arthritis-driving type I IFN that is regulated by a locus, *Bbaa1,* previously identified by forward genetics (Fig. 1). This culminates a decade of our work wherein two parallel pathways of investigation revealed a pathologic type I IFN profile in C3H mice infected with *B. burgdorferi* that is suppressed by IFNAR1 blockade (14, 18–22). Others have corroborated the association between pathologic type I IFN production and Lyme disease pathogenesis in murine studies (52, 53) as well as in human patients at various stages of disease (2, 24), and many investigators have examined the type I IFN response to *B. burgdorferi* in murine and human cells (19, 20, 43, 53–62). But

the exact pathogenic member has remained elusive due to the transient expression of IFN-α/β (63, 64), overlapping interferon-stimulated gene pathways induced by IFN-α/β (65), and differing contexts of *B. burgdorferi* infection in which IFN-α/β transcripts have been detected. The strength of this study centers on the employment of B6.C3-*Bbaa1* mice, which allowed the impact of type I IFN dysregulation to be assessed in isolation from the five other *B. burgdorferi* arthritis-associated QTL contained within the C3H genome (21), coupled with the use of newly available mAbs to assess IFN-α and IFN-β individually.

Multiple mAb experiments along with the transcriptional detection of *Ifnb* in BMDMs from refined congenic lines (and lack of evidence for *Ifna* transcripts) revealed that IFN-β is the sole contributor to the type I IFN profile and arthritogenesis in *Bbaa1*-directed Lyme arthritis (Fig. 1, 2). Another major finding was that partial control of IFN-β is intrinsic to the *Bbaa1* locus (Fig. 4, 5). The intrinsic regulation of IFN-β within *Bbaa1* was surprising due to the lack of coding or regulatory SNPs within 10,000 flanking base pairs of the *Ifnb* genetic sequence (66, 67) and suggests a novel mechanism for IFN-β regulation, which is a topic of future investigation. Here, the congenic mice provided a unique tool to segregate IFN-β initiation from feed-forward amplification, and radiation chimeras demonstrated that the *Bbaa1* arthritis-initiating lineage is radiation-sensitive in the joint (Fig. 3). This finding is in contrast to our previous publication on the *Bbaa2* QTL, in which the hypomorphic allele of *Gusb* drives arthritis through accumulation of glycosaminoglycans in the radiation-resistant resident joint population (23). Thus, our forward genetic approach has identified two distinct QTLs that regulate Lyme arthritis through independent mechanisms and responsible initiating cell lineages.

In the case of *Bbaa1,* the discrimination among cell types along with refined congenic lines was critical to understanding the mechanism of arthritis development. An unbiased RNA-seq on resident ($CD45^{-}$) joint cells led to the third major finding that IFN-β acting as an eQTL underlying *Bbaa1* regulates myostatin expression (Fig. 6, 7, Table I). This was surprising given that myostatin is widely appreciated for its role as a negative regulator of skeletal muscle growth and regeneration (68), and intensely investigated for its positive impact on food production in the animal agriculture industry. Nevertheless, we were able to utilize a newly developed reagent in the field of muscle development to inhibit myostatin protein activity *in vivo* and discovered that myostatin is a direct mediator of *Bbaa1* Lyme arthritis development (Fig. 8, Supplemental Fig. 4). Strikingly, myostatin was recently found to be a mediator of a distinct inflammatory arthritis using the TNF-α overexpression model of RA in mice, and found to be expressed by synovial fibroblasts from patients with RA (50).

We do not currently have a complete picture of the means by which the IFN-β to myostatin axis results in Lyme arthritis development, and find it surprising that myostatin is not encoded by any of the QTL previously identified by forward genetics between B6 and C3H mice (14, 21). Clearly the impact of IFN-β on the pathogenesis of Lyme disease involves a complex web, and the development of congenic mice with reduced physical intervals provides a unique tool for identifying tissue specific components of pathogenesis. Of great interest is the recent demonstration that myostatin promotes RA in TNF-α overexpressing mice by activating osteoclast differentiation (50). Although bone pathologies have not been widely investigated in Lyme arthritis patients or mice, Tang *et al.* recently identified *B.*

burgdorferi infection in mice bone, and found that inhibition of osteoblast activity lead to bone destruction (69). Because *B. burgdorferi* also infects quadriceps muscle (70, 71), our identification of myostatin suggests that a more global involvement of bone and muscle in the response to *B. burgdorferi* may be involved in Lyme arthritis development than previously appreciated. Future studies are needed to investigate the role of myostatin in bone and other tissues of the joint on Lyme arthritis development and the ability to reverse clinical disease once established.

This paper capitalized on the power of forward genetics in studying pathogenesis in an animal model, wherein refined congenic lines afforded the opportunity to assess transcriptional differences limited to extremely narrow genomic differences using RNA-seq, and radiation chimeras illuminated the “hand off” of cells involved in arthritis development. Additionally, myostatin is not encoded within the *Bbaa1* QTL, illuminating the vast potential of control exerted by this limited genetic region. Future studies will be directed on delineating the important sources and inflammatory targets of myostatin *in vivo*, which could uncover unrecognized signaling pathways in this inflammatory arthritis. Myostatin directed therapies are an appealing distinction from classic anti-inflammatory targets, as anti-bacterial responses are expected to remain intact. Additionally, myostatin inhibition is currently in various stages of clinical trials for patients with muscle wasting conditions and receiving attention as a potential therapeutic target for many metabolic disorders (68), studies which could provide insight into potential for inflammatory disorders such as arthritis as well.

Supplementary Material

Refer to Web version on PubMed Central for supplementary material.

Acknowledgments

Grant support:

National Institutes of Health/National Institute of Arthritis and Musculoskeletal and Skin Diseases grant AR043521 (to J.J.W. and C.T.). National Institutes of Health/National Institute of Allergy and Infectious Disease grants AI032223 and AI1114462 (to J.J.W.), and AI128595 (to C.T.). National Institutes of Health/National Institute of Neurological Disorders and Stroke grant NS095007 (to C.T.). National Multiple Sclerosis Society (NMSS) grant RG5170A6 (to C.T.). USDA-NIFA grant 2010-34135-21229 (to Y.S.K.).

We thank Scott Hale, Dean Tantin, and members of the Weis laboratory for helpful discussions during the course of these studies. Thank you also to Brian Dalley and the High Throughput Genomics Core Facility for expert guidance and for performing the RNA-seq, and Chris Stubben in the High Throughput Genomics Core Facility for analyzing the sequencing data. Thank you also to Anna Dilger at the University of Illinois at Urbana-Champaign for insightful discussions on myostatin inhibitory reagents.

Abbreviations

B6	C57BL/6
Bbaa	Borrelia burgdorferi arthritis-associated locus
BMDM	bone marrow-derived macrophage
eQTL	expression quantitative trait locus

IFNAR1	IFN-α/β receptor subunit 1
ISRCL	interval specific recombinant congenic line
QTL	quantitative trait locus
RA	rheumatoid arthritis

References

1. Kuehn BM. CDC estimates 300,000 US cases of Lyme disease annually. JAMA. 2013; 310:1110. [PubMed: 24045727]
2. Jacek E, Fallon BA, Chandra A, Crow MK, Wormser GP, Alaedini A. Increased IFNα activity and differential antibody response in patients with a history of Lyme disease and persistent cognitive deficits. J Neuroimmunol. 2013; 255:85–91. [PubMed: 23141748]
3. Yoon EC, Vail E, Kleinman G, Lento Pa, Li S, Wang G, Limberger R, Fallon JT. Lyme disease: a case report of a 17-year-old male with fatal Lyme carditis. Cardiovasc Pathol. 2015:2–6.
4. Centers for Disease Control and Prevention. Three sudden cardiac deaths associated with Lyme carditis — United States, November 2012 – July 2013. Morb Mortal Wkly Rep. 2013; 62:993–1018.
5. Borchers A, Keen C, Huntley A, Gershwin ME. Lyme disease: a rigorous review of diagnostic criteria and treatment. J Autoimmun. 2015; 57:82–115. [PubMed: 25451629]
6. Steere AC, Glickstein L. Elucidation of Lyme arthritis. Nat Rev Immunol. 2004; 4:143–152. [PubMed: 15040587]
7. Steere AC, Schoen RT, Taylor E. The clinical evolution of Lyme arthritis. Ann Intern Med. 1987; 107:725–731. [PubMed: 3662285]
8. Petzke M, Schwartz I. *Borrelia burgdorferi* pathogenesis and the immune response. Clin Lab Med. 2015; 35:745–764. [PubMed: 26593255]
9. Steere AC, Dwyer E, Winchester R. Association of chronic Lyme arthritis with HLA-DR4 and HLA-DR2 alleles. N Engl J Med. 1990; 323:219–223. [PubMed: 2078208]
10. Schröder NWJ, Diterich I, Zinke A, Eckert J, Draing C, Baehr V, Hassler D, Priem S, Hahn K, Michelsen KS, Hartung T, Burmester GR, Göbel UB, Hermann C, Schumann RR. Heterozygous Arg753Gln polymorphism of human TLR-2 impairs immune activation by *Borrelia burgdorferi* and protects from late stage Lyme disease. J Immunol. 2005; 175:2534–2540. [PubMed: 16081826]
11. Steere AC, Klitz W, Drouin EE, Falk BA, Kwok WW, Nepom GT, Baxter-Lowe LA. Antibiotic-refractory Lyme arthritis is associated with HLA-DR molecules that bind a *Borrelia burgdorferi* peptide. J Exp Med. 2006; 203:961–971. [PubMed: 16585267]
12. Strle K, Shin JJ, Glickstein LJ, Steere AC. Association of a toll-like receptor 1 polymorphism with heightened Th1 inflammatory responses and antibiotic-refractory Lyme arthritis. Arthritis Rheum. 2012; 64:1497–1507. [PubMed: 22246581]
13. Barthold SW, Beck DS, Hansen GM, Terwilliger GA, Moody KD. Lyme borreliosis in selected strains and ages of laboratory mice. J Infect Dis. 1990; 162:133–138. [PubMed: 2141344]
14. Weis JJ, McCracken BA, Ma Y, Fairbairn D, Roper RJ, Morrison TB, Weis JH, Zachary JF, Doerge RW, Teuscher C. Identification of quantitative trait loci governing arthritis severity and humoral responses in the murine model of Lyme disease. J Immunol. 1999; 162:948–956. [PubMed: 9916719]
15. Roper RJ, Weis JJ, McCracken BA, Green CB, Ma Y, Weber KS, Fairbairn D, Butterfield RJ, Potter MR, Zachary JF, Doerge RW, Teuscher C. Genetic control of susceptibility to experimental Lyme arthritis is polygenic and exhibits consistent linkage to multiple loci on chromosome 5 in four independent mouse crosses. Genes Immun. 2001; 2:388–397. [PubMed: 11704805]
16. Ray A, Kumar D, Shakya A, Brown CR, Cook JL, Ray BK. Serum amyloid A-activating factor-1 (SAF-1) transgenic mice are prone to develop a severe form of inflammation-induced arthritis. J Immunol. 2004; 173:4684–4691. [PubMed: 15383604]

17. Blaho, Va, Mitchell, WJ., Brown, CR. Arthritis develops but fails to resolve during inhibition of cyclooxygenase 2 in a murine model of Lyme disease. Arthritis Rheum. 2008; 58:1485–1495. [PubMed: 18438879]

18. Crandall H, Dunn DM, Ma Y, Wooten RM, Zachary JF, Weis JH, Weiss RB, Weis JJ. Gene expression profiling reveals unique pathways associated with differential severity of Lyme arthritis. J Immunol. 2006; 177:7930–7942. [PubMed: 17114465]

19. Miller JC, Ma Y, Bian J, Sheehan KCF, Zachary JF, Weis JH, Schreiber RD, Weis JJ. A critical role for type I IFN in arthritis development following *Borrelia burgdorferi* infection of mice. J Immunol. 2008; 181:8492–8503. [PubMed: 19050267]

20. Lochhead RB, Sonderegger FL, Ma Y, Brewster E, Cornwall D, Maylor-Hagen H, Miller JC, Zachary JF, Weis JH, Weis JJ. Endothelial cells and fibroblasts amplify the arthritogenic type I IFN response in murine Lyme disease and are major sources of chemokines in *Borrelia burgdorferi*-infected joint tissue. J Immunol. 2012; 189:2488–2501. [PubMed: 22851707]

21. Ma Y, Miller JC, Crandall H, Larsen ET, Dunn DM, Weiss RB, Subramanian M, Weis JH, Zachary JF, Teuscher C, Weis JJ. Interval-specific congenic lines reveal quantitative trait loci with penetrant Lyme arthritis phenotypes on chromosomes 5, 11, and 12. Infect Immun. 2009; 77:3302–3311. [PubMed: 19487472]

22. Ma Y, Bramwell KKC, Lochhead RB, Paquette JK, Zachary JF, Weis JH, Weis JJ. *Borrelia burgdorferi* arthritis-associated locus *Bbaa1* regulates Lyme arthritis and K/B×N serum transfer arthritis through intrinsic control of type I IFN production. J Immunol. 2014; 193:6050–6060. [PubMed: 25378596]

23. Bramwell KKC, Ma Y, Weis JH, Chen X, Zachary JF, Teuscher C, Weis JJ. Lysosomal β-glucuronidase regulates Lyme and rheumatoid arthritis severity. J Clin Invest. 2014; 124:311–320. [PubMed: 24334460]

24. Salazar JC, Pope CD, Sellati TJ, Feder HM Jr, Caimano MJ, Pope JG, Krause PJ, Radolf JD. Coevolution of markers of innate and adaptive immunity in skin and peripheral blood of patients with erythema migrans. J Immunol. 2003; 171:2660–2670. [PubMed: 12928420]

25. van der Pouw Kraan TCTM, Wijbrandts CA, van Baarsen LGM, Voskuyl AE, Rustenburg F, Baggen MJ, Ibrahim SM, Fero M, Dijkmans BAC, Tak PP, Verweij CL. Rheumatoid arthritis subtypes identified by genomic profiling of peripheral blood cells: assignment of a type I interferon signature in a subpopulation of patients. Ann Rheum Dis. 2007; 66:1008–1014. [PubMed: 17223656]

26. Wilson LE, Widman D, Dikman SH, Gorevic PD. Autoimmune disease complicating antiviral therapy for hepatitis C virus infection. Semin Arthritis Rheum. 2002; 32:163–173. [PubMed: 12528081]

27. Vilcek J. Fifty years of interferon research: aiming at a moving target. Immunity. 2006; 25:343–348. [PubMed: 16979566]

28. Bramwell KKC, Weis JH, Teuscher C, Weis JJ. High-throughput genotyping of advanced congenic lines by high resolution melting analysis for identificaton of *Bbaa2*, a QTL controlling Lyme arthritis. Biotechniques. 2012; 52:183–190. [PubMed: 22401552]

29. Barthold SW, Persing DH, Armstrong AL, Peeples RA. Kinetics of *Borrelia burgdorferi* dissemination and evolution of disease after intradermal inoculation of mice. Am J Pathol. 1991; 139:263–273. [PubMed: 1867318]

30. Brown JP, Zachary JF, Teuscher C, Weis JJ, Wooten RM. Dual role of interleukin-10 in murine Lyme disease: regulation of arthritis severity and host defense. Infect Immun. 1999; 67:5142–5150. [PubMed: 10496888]

31. Wooten RM, Ma Y, Yoder RA, Jeanette P, Weis JH, Zachary JF, Kirschning CJ, Weis JJ. Toll-Like receptor 2 is required for innate, but not acquired, host defense to *Borrelia burgdorferi*. J Immunol. 2002; 168:348–355. [PubMed: 11751980]

32. Ornstein K, Barbour AG. A reverse-transcriptase-polymerase chain reaction assay of *Borrelia burgdorferi* 16S rRNA for highly sensitive quantification of pathogen load in a vector. Vector Borne Zootonic Dis. 2006; 6:103–112.

33. Morrison TB, Ma Y, Weis JH, Weis JJ. Rapid and sensitive quantification of *Borrelia burgdorferi*-infected mouse tissues by continuous fluorescent monitoring of PCR. J Clin Microbiol. 1999; 37:987–992. [PubMed: 10074514]
34. Sheehan KCF, Lazear HM, Diamond MS, Schreiber RD. Selective blockade of interferon-α and -β reveals their non-redundant functions in a mouse model of West Nile virus infection. PLoS One. 2015; 10:1–19.
35. Sheehan KCF, Lai KS, Dunn GP, Bruce AT, Diamond MS, Heutel JD, Dungo-Arthur C, Carrero JA, White JM, Hertzog PJ, Schreiber RD. Blocking monoclonal antibodies specific for mouse IFN-α/β receptor subunit 1 (IFNAR-1) from mice immunized by in vivo hydrodynamic transfection. J Interf Cytokine Res. 2006; 26:804–819.
36. Lee SB, Kim JH, Jin DH, Jin HJ, Kim YS. Myostatin inhibitory region of fish (Paralichthys olivaceus) myostatin-1 propeptide. Comp Biochem Physiol Part B Biochem Mol Biol. 2016; 194–195:65–70.
37. Sonderegger FL, Ma Y, Maylor-Hagan H, Brewster J, Huang X, Spangrude GJ, Zachary JF, Weis JH, Weis JJ. Localized production of IL-10 suppresses early inflammatory cell infiltration and subsequent development of IFN-γ– mediated Lyme arthritis. J Immunol. 2012; 188:1381–1393. [PubMed: 22180617]
38. Meerpohl H, Lohmann-Matthes M, Fischer H. Studies on the activation of mouse bone marrow-derived macrophages by the macrophage cytotoxicity factor (MCF). Eur J Immunol. 1976; 6:213–217. [PubMed: 1086777]
39. Krutzik PO, Nolan GP. Intracellular phospho-protein staining techniques for flow cytometry: monitoring single cell signaling events. Cytometry. 2003; 55A:61–70.
40. Dobin A, Davis CA, Schlesinger F, Drenkow J, Zaleski C, Jha S, Batut P, Chaisson M, Gingeras TR. STAR: ultrafast universal RNA-seq aligner. Bioinformatics. 2013; 29:15–21. [PubMed: 23104886]
41. Liao Y, Smyth GK, Shi W. featureCounts: an efficient general purpose program for assigning sequence reads to genomic features. Bioinformatics. 2014; 30:923–930. [PubMed: 24227677]
42. Love MI, Huber W, Anders S. Moderated estimation of fold change and dispersion for RNA-seq data with DESeq2. Genome Biol. 2014; 15:1–21.
43. Miller JC, Maylor-hagen H, Ma Y, John H, Weis JJ, Miller JC, Maylor-hagen H, Ma Y, Weis JH, Weis JJ. The Lyme disease spirochete *Borrelia burgdorferi* utilizes multiple ligands, including RNA, for interferon regulatory factor 3-dependent induction of type I interferon-responsive genes. Infect Immun. 2010; 78:3144–3153. [PubMed: 20404081]
44. Ma Y, Seiler KP, Tai KF, Yang L, Woods M, Weis JJ. Outer surface lipoproteins of *Borrelia burgdorferi* stimulate nitric oxide production by the cytokine-inducible pathway. Infect Immun. 1994; 62:3663–3671. [PubMed: 7520417]
45. Ng CT, Sullivan BM, Teijaro JR, Lee AM, Welch M, Rice S, Sheehan KCF, Schreiber RD, Oldstone MBA. Blockade of interferon beta, but not interferon alpha, signaling controls persistent viral infection. Cell Host Microbe. 2015; 17:653–661. [PubMed: 25974304]
46. Bolz DD, Sundsbak RS, Ma Y, Kirschning CJ, Zachary JF, John H, Weis JJ. MyD88 plays a unique role in host defense but not arthritis development in Lyme disease. J Immunol. 2004; 173:2003–2010. [PubMed: 15265935]
47. Liu N, Montgomery RR, Barthold SW, Bockenstedt LK. Myeloid differentiation antigen 88 deficiency impairs pathogen clearance but does not alter inflammation in *Borrelia burgdorferi*-infected mice. Infect Immun. 2004; 72:3195–3203. [PubMed: 15155621]
48. Ivashkiv LB, Donlin LT. Regulation of type I interferon responses. Nat Rev Immunol. 2014; 14:36–49. [PubMed: 24362405]
49. Brown CR V, Blaho A, Fritsche KL, Loiacono CM. Stat1 deficiency exacerbates carditis but not arthritis during experimental Lyme borreliosis. J Interf Cytokine Res. 2006; 26:390–399.
50. Dankbar B, Fennen M, Brunert D, Hayer S, Frank S, Wehmeyer C, Beckmann D, Paruzel P, Bertrand J, Redlich K, Koers-Wunrau C, Stratis A, Korb-Pap A, Pap T. Myostatin is a direct regulator of osteoclast differentiation and its inhibition reduces inflammatory joint destruction in mice. Nat Med. 2015; 21:1085–1090. [PubMed: 26236992]

51. Li Z, Zhao B, Kim YS, Hu CY, Yang J. Administration of a mutated myostatin propeptide to neonatal mice significantly enhances skeletal muscle growth. Mol Reprod Dev. 2010; 77:76–82. [PubMed: 19743472]
52. Hastey CJ, Ochoa J, Olsen KJ, Barthold SW, Baumgarth N. MyD88- and TRIF-independent induction of type I interferon drives naive B cell accumulation but not loss of lymph node architecture. Infect Immun. 2014; 82:1548–1558. [PubMed: 24452685]
53. Petzke MM, Iyer R, Love AC, Spieler Z, Brooks A, Schwartz I. *Borrelia burgdorferi* induces a type I interferon response during early stages of disseminated infection in mice. BMC Microbiol. 2016; 16:1–13. [PubMed: 26728027]
54. Cervantes JL, La Vake CJ, Weinerman B, Luu S, Connell CO, Verardi PH, Salazar JC. Human TLR8 is activated upon recognition of *Borrelia burgdorferi* RNA in the phagosome of human monocytes. J Leukoc Biol. 2013; 94:1231–1241. [PubMed: 23906644]
55. Love AC, Schwartz I, Petzke MM. *Borrelia burgdorferi* RNA induces type I and III interferons via toll-like receptor 7 and contributes to production of NF-kB-dependent cytokines. Infect Immun. 2014; 82:2405–2416. [PubMed: 24664510]
56. Krupna-Gaylord MA, Liveris D, Love AC, Wormser GP, Schwartz I, Petzke MM. Induction of type I and type III interferons by *Borrelia burgdorferi* correlates with pathogenesis and requires linear plasmid 36. PLoS One. 2014; 9:1–14.
57. Petnicki-Ocwieja T, Defrancesco AS, Chung E, Darcy CT, Bronson RT, Kobayashi KS, Hu LT. Nod2 suppresses *Borrelia burgdorferi* mediated murine Lyme arthritis and carditis through the induction of tolerance. PLoS One. 2011; 6:1–13.
58. Salazar JC, Duhnam-Ems S, La Vake C, Cruz AR, Moore MW, Caimano MJ, Velez-Climent L, Shupe J, Krueger W, Radolf JD. Activation of human monocytes by live *Borrelia burgdorferi* generates TLR2-dependent and -independent responses which include induction of IFN-β. PLoS Pathog. 2009; 5:1–21.
59. Dietrich N, Lienenklaus S, Weiss S, Gekara NO. Murine toll-like receptor 2 activation induces type I interferon responses from endolysosomal compartments. PLoS One. 2010; 5:1–10.
60. Petnicki-Ocwieja T, Chung E, Acosta DI, Ramos LT, Shin OS, Ghosh S, Kobzik L, Li X, Hu LT. TRIF mediates toll-like receptor 2-dependent inflammatory responses to *Borrelia burgdorferi*. Infect Immun. 2013; 81:402–410. [PubMed: 23166161]
61. Cervantes JL, Dunham-Ems SM, La Vake CJ, Petzke MM, Sahay B, Sellati TJ, Radolf JD, Salazar JC. Phagosomal signaling by *Borrelia burgdorferi* in human monocytes involves Toll-like receptor (TLR) 2 and TLR8 cooperativity and TLR8-mediated induction of IFN-β. Proc Natl Acad Sci USA. 2011; 108:3683–3688. [PubMed: 21321205]
62. Petzke MM, Brooks A, Krupna MA, Mordue D, Schwartz I. Recognition of *Borrelia burgdorferi*, the Lyme disease spirochete, by TLR7 and TLR9 induces a type I IFN response by human immune cells. J Immunol. 2009; 183:5279–5292. [PubMed: 19794067]
63. Schreiber G, Piehler J. The molecular basis for functional plasticity in type I interferon signaling. Trends Immunol. 2015; 36:139–149. [PubMed: 25687684]
64. Schreiber G. The molecular basis for differential type I interferons signaling. J Biol Chem. 2017:1–18. [PubMed: 27881675]
65. Schneider WM, Chevillotte MD, Rice CM. Interferon-stimulated genes: a complex web of host defenses. Annu Rev Immunol. 2014; 32:513–545. [PubMed: 24555472]
66. Keane TM, Goodstadt L, Danecek P, White MA, Wong K, Yalcin B, Heger A, Agam A, Slater G, Goodson M, Furlotte NA, Eskin E, Nellåker C, Whitley H, Cleak J, Janowitz D, Hernandez-Pliego P, Edwards A, Belgard TG, Oliver PL, McIntyre RE, Bhomra A, Nicod J, Gan X, Yuan W, van der Weyden L, Steward CA, Balasubramaniam S, Stalker J, Mott R, Durbin R, Jackson IJ, Czechanski A, Afonso J, Assuncao G, Donahue LR, Reinholdt LG, Payseru BA, Ponting CP, Briney E, Flint J, Adams DJ. Mouse genomic variation and its effect on phenotypes and gene regulation. Nature. 2011; 477:289–294. [PubMed: 21921910]
67. Yalcin B, Wong K, Agam A, Goodson M, Keane TM, Gan X, Nellåker C, Goodstadt L, Nicod J, Bhomra A, Hernandez-Pliego P, Whitley H, Cleak J, Dutton R, Janowitz D, Mott R, Adams DJ, Flint J. Sequence based characterization of structural variation in the mouse genome. Nature. 2011; 477:326–329. [PubMed: 21921916]

68. Sharma M, Mcfarlane C, Kambadur R, Kukreti H, Bonala S, Srinivasan S. Myostatin: expanding horizons. Biochem Mol Bio Int. 2015; 67:589–600.

69. Tang TT, Zhang L, Bansal A, Grynpas M, Moriarty TJ. The Lyme disease pathogen *Borrelia burgdorferi* infects murine bone and induces trabecular bone loss. Infect Immun. 2017; 85:1–13.

70. Hodzic E, Feng S, Freet KJ, Barthold SW. *Borrelia burgdorferi* population dynamics and prototype gene expression during infection of immunocompetent and immunodeficient mice. Infect Immun. 2003; 71:5042–5055. [PubMed: 12933847]

71. Hodzic E, Feng S, Barthold SW. Assessment of transcriptional activity of *Borrelia burgdorferi* and host cytokine genes during early and late infection in a mouse model. Vector Borne Zootonic Dis. 2013; 13:694–711.

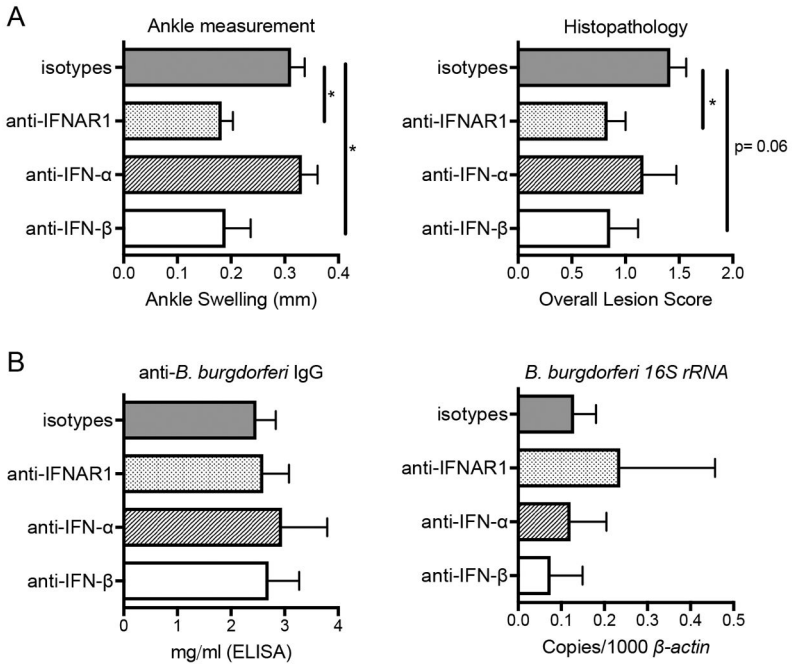

FIGURE 1.

Blocking of IFN-β in B6.C3-*Bbaa1* mice suppresses Lyme arthritis to the same extent as blocking IFNAR1. B6.C3-*Bbaa1* mice were infected with 2×10^4 *B. burgdorferi* and treated with anti-IFNAR1 (MAR1-5A3), anti-IFN-α (TIF-3C5) or anti-IFN-β (HDβ-4A7) as described in *Materials and Methods* ($n = 5$ to 6 mice per group). (**A**) Arthritis was assessed 4 wk post infection, and shown for change in ankle measurement and overall lesion scores. (**B**) Host defense was assessed by anti-*B. burgdorferi* IgG in the serum and *B. burgdorferi 16S rRNA* transcripts in the joint. Statistical significance for ankle swelling, serum IgG, and bacterial numbers in the joint were determined by 1-way ANOVA followed by Dunnett's multiple comparison test versus isotype, and Mann-Whitney *U* test was used for overall lesion. *$p < 0.05$.

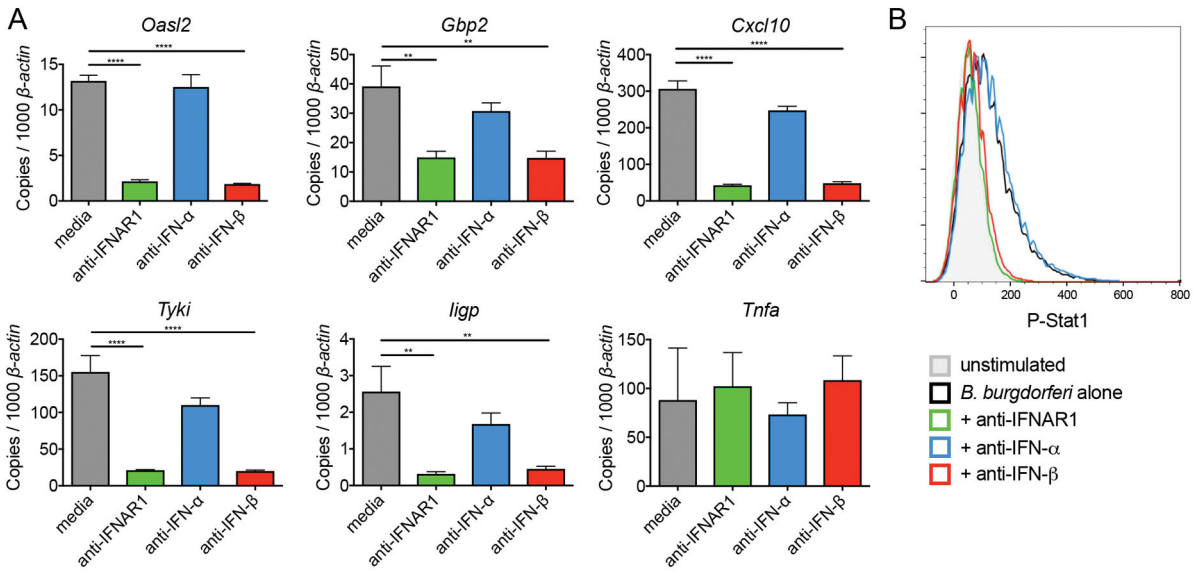

FIGURE 2.

IFN-β drives the type I IFN profile in B6.C3-*Bbaa1* BMDMs stimulated with *B. burgdorferi*. (**A**) qRT-PCR analysis of transcripts after 6 h stimulation with live *B. burgdorferi* (10:1 MOI) and treatment with anti-IFNAR1, anti-IFN-α, or anti-IFN-β (10 μg/ml each). Transcript levels for *Oasl2, Gbp2, Cxcl10, Tyki, Iigp,* and *Tnfa* were normalized to *β-actin*. Data are pooled from two experiments conducted on separate days ($n = 4$ per group). Significance determined by 1-way ANOVA followed by Dunnett's multiple comparison test versus media. *$p < 0.05$, **$p < 0.01$, ***$p < 0.001$, ****$p < 0.0001$. (**B**) Flow cytometric analysis of Stat-1 phosphorylation after 15 h stimulation with *B. burgdorferi* and treatment with blocking antibodies. Data are representative of three independent experiments.

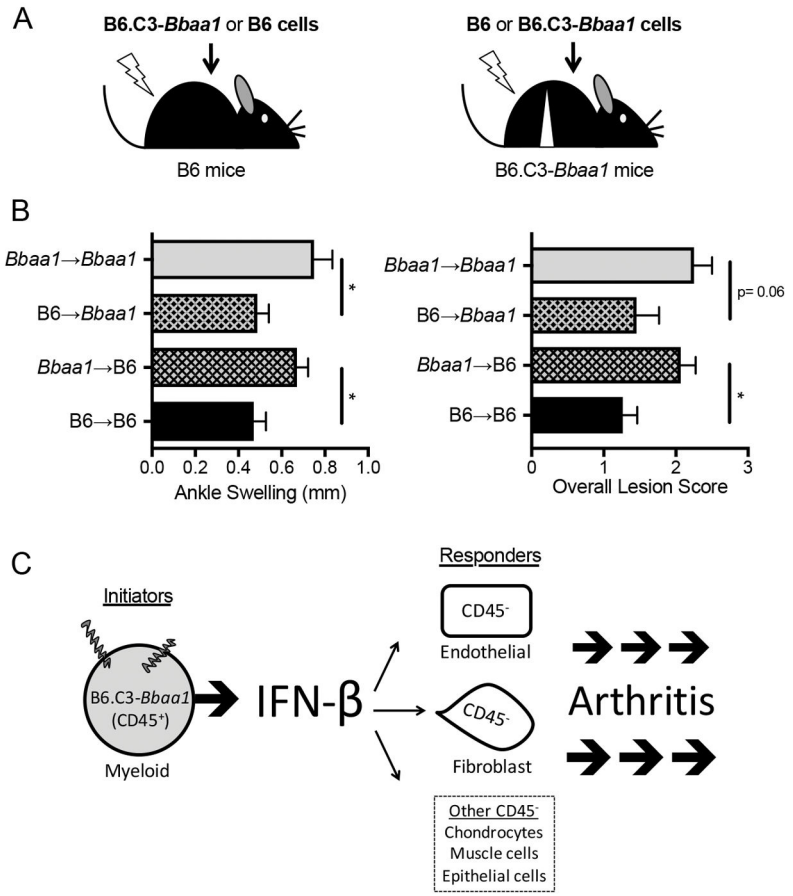

FIGURE 3.

Radiation chimeras between B6 and B6.C3-*Bbaa1* mice identify distinct roles for radiation resistant and radiation sensitive lineages in arthritis development. (**A**) Experimental design: following a lethal dose of irradiation, B6 mice were reconstituted with B6.C3-*Bbaa1* splenocytes (*Bbaa1*→B6) and B6.C3-*Bbaa1* mice were reconstituted with B6 splenocytes (B6→*Bbaa1*). Autologous transplants (B6→B6 and *Bbaa1*→*Bbaa1*) were also generated for impact of myeloablative radiation. Arrows indicate direction of transplantation from donor to recipient. (**B**) *Bbaa1* influences arthritis severity through the radiosensitive hematopoietic lineage. Notably, *Bbaa1*→B6 mice developed the full Lyme arthritis phenotype while B6→*Bbaa1* mice were resistant. Arthritis measurements were taken 4 wk post infection with *B. burgdorferi* (n = 8 to 19 mice per group). Statistical significance was assessed between mice of the same recipient genotype by Student's t test for ankle swelling and Mann-Whitney U test for overall lesion. *$p < 0.05$. (**C**) Model depicting the cellular "pass off" between radiosensitive myeloid ($CD45^+$) cells that initiate IFN-β in response to *B. burgdorferi* and radioresistant resident ($CD45^-$) cells that respond to IFN-β and drive arthritis development.

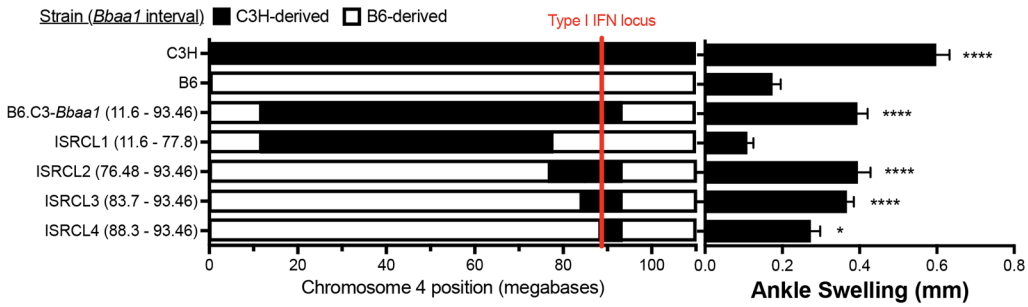

FIGURE 4.

Physical boundaries of *Bbaa1* advanced congenic intervals (left) and Lyme arthritis (right) reveal inclusion of the C3H allele for the type I IFN cluster and flanking genes are required for increased arthritis phenotype. Parentheses indicate the exact interval of each congenic line, and rows represent the genetic composition across Chr4, with C3H-derived regions shaded black and B6-derived regions in white. Arthritis shown for ankle swelling measured 4 wk after *B. burgdorferi* infection (n = 10 to 35 mice per group). Significance assessed by 1-way ANOVA followed by Dunnett's multiple comparison test versus B6. *$p < 0.05$, ****$p < 0.0001$.

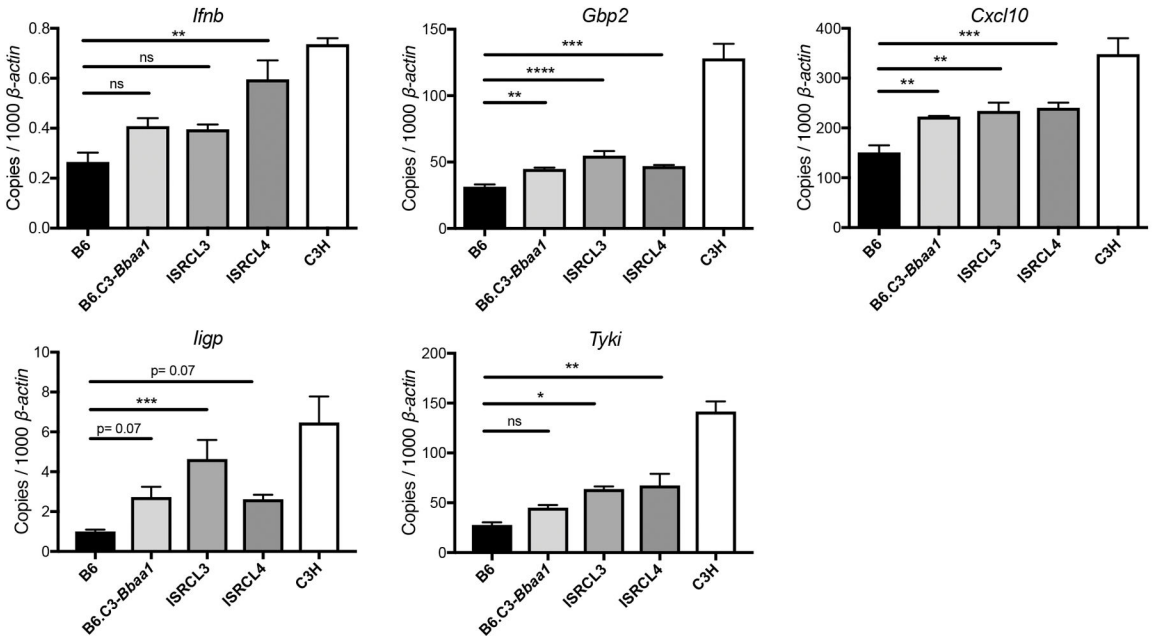

FIGURE 5.

BMDMs demonstrate that genes within *Bbaa1* intervals of ISRCL3 and ISRCL4 partially regulate the magnitude of the IFN response to *B. burgdorferi*. qRT-PCR analysis of transcripts in BMDMs from B6, B6.C3-*Bbaa1,* ISRCL3, ICRCL4, and C3H mice stimulated with live *B. burgdorferi* for 6 h ($n = 3$ to 4 per group). Transcript levels for *Ifnb, Gbp2, Cxcl10, Iigp,* and *Tyki* were normalized to *β-actin*. Significance for differences between congenic lines and B6 was determined by 1-way ANOVA followed by Dunnett's multiple comparison test. *$p < 0.05$, **$p < 0.01$, ***$p < 0.001$, ****$p < 0.0001$.

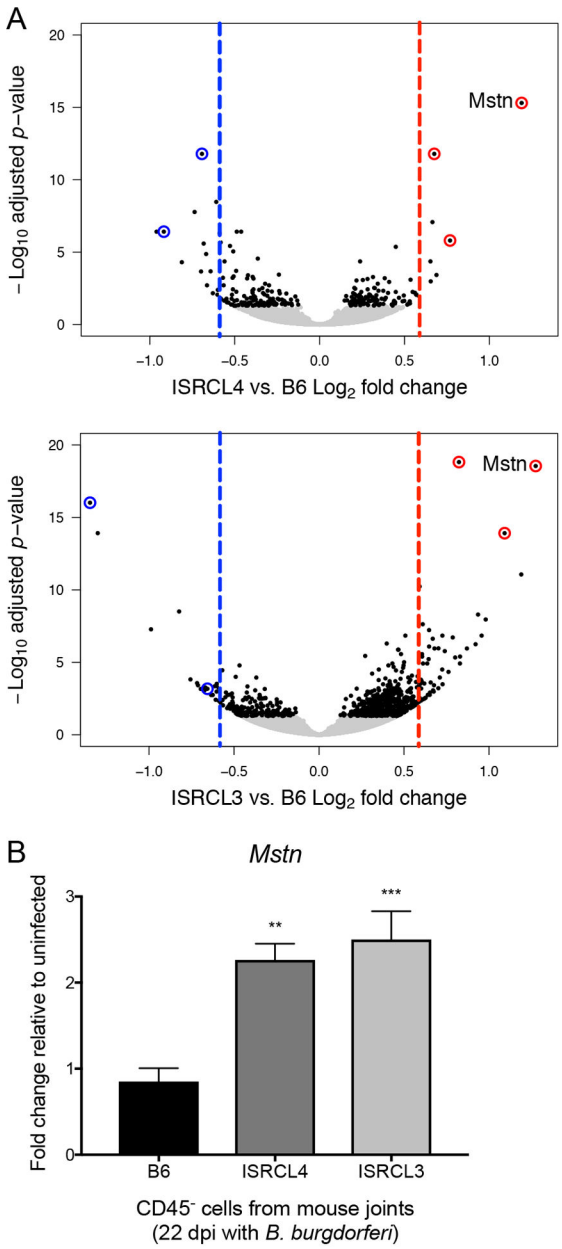

FIGURE 6.

RNA-seq identification of myostatin (*Mstn*) as a candidate for *Bbaa1*-directed Lyme arthritis development. (**A**) Volcano plot depicts $\log_2$ fold change (*x*-axis) and $-\log_{10}$ adjusted *p*-value (*y*-axis) of genes identified by ISRCL4 vs. B6 and ISRCL3 vs. B6 RNA-seq comparisons. Single genes are plotted as dots, with those achieving significance (*p*-adj <0.05) colored black (*n* = 5 samples per genotype, each sample was comprised of cells from both rear ankle joints pooled from two mice). Red and blue dashed lines mark 1.5-fold increase in the congenic or B6, respectively. Circled genes had ≥ 1.5-fold change and *p*-adj <0.05 in both comparisons. (**B**) qRT-PCR analysis of *Mstn* expression in $CD45^-$ cells isolated from a distinct group of B6, ISRCL4, and ISRCL3 mice infected with *B. burgdorferi* for 22 days (*n* = 5 to 6 per group). *Mstn* transcripts were normalized to *β-actin* and fold change relative to

uninfected levels were calculated for each strain. Significance assessed by 1-way ANOVA followed by Dunnett's multiple comparison test versus B6. $^{**}p < 0.01$, $^{***}p < 0.001$.

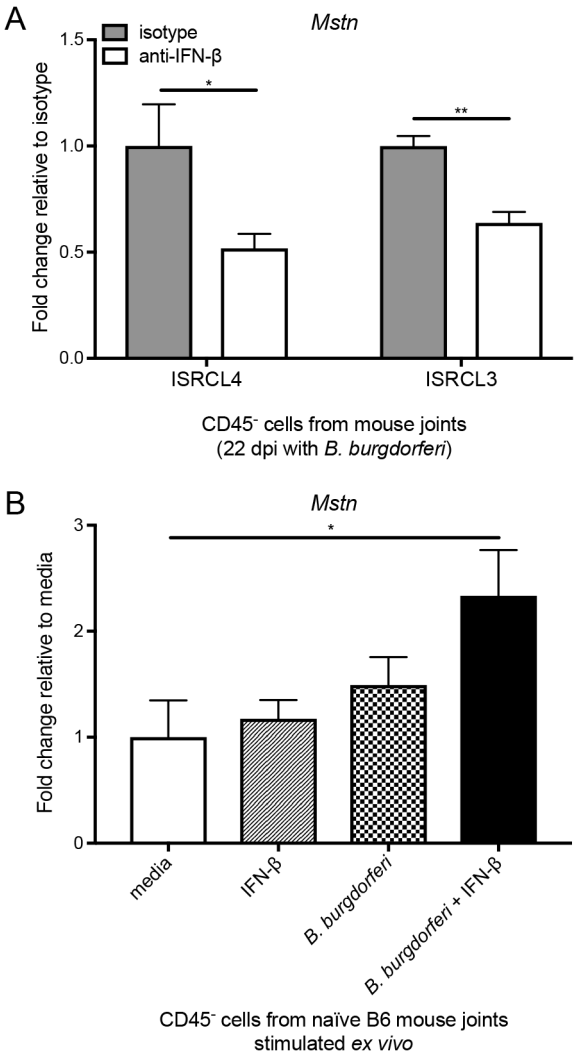

FIGURE 7.

IFN-β and *B. burgdorferi* are both required for the enhanced expression of myostatin by CD45⁻ joint cells during infection and *ex vivo*. (**A**) *In vivo* mAb blocking of IFN-β (600 μg total) prevents transcriptional upregulation of *Mstn* in CD45⁻ joint cells from ISRCL4 and ISRCL3 mice 22 days post infection with *B. burgdorferi* ($n = 3$ to 4 samples per group, each sample was comprised of cells from both rear ankle joints pooled from two mice). *Mstn* transcripts were normalized to *β-actin* and fold change relative to isotype control was calculated for each strain. Significance determined by unpaired Student's *t* test. $*p < 0.05$, $**p < 0.01$. (**B**) *Ex vivo* administration of exogenous IFN-β (100 U/ml) in combination with *B. burgdorferi* (10:1 MOI) for 3 h caused transcriptional upregulation of *Mstn* in CD45⁻ cells isolated from a naïve B6 mouse joint. Transcripts were normalized to *β-actin* and fold change was calculated relative to media control. Results are pooled data from two experiments using CD45⁻ cells from 8 or more mice done on separate days ($n = 5$ wells per group). Significance determined by 1-way ANOVA followed by Dunnett's multiple comparison test versus media. $*p < 0.05$.

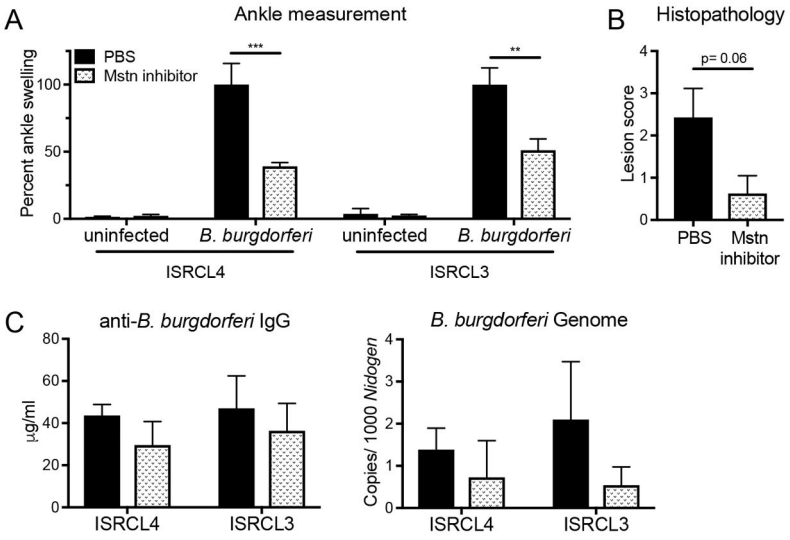

FIGURE 8.

Myostatin inhibition suppresses the development of Lyme arthritis in *Bbaa1* congenic mice. ISRCL4 and ISRCL3 mice were infected with 2×10^4 *B. burgdorferi* and treated with a myostatin inhibitor as described in *Materials and Methods* ($n = 3$ to 4 mice per group). Arthritis was assessed 4 wk post infection, and shown for (**A**) ankle swelling relative to infected PBS treated animals for each genotype and (**B**) histopathological lesion scores of infected congenic lines. (**C**) Host defense was assessed by anti-*B. burgdorferi* IgG in the serum and qRT-PCR quantification of *B. burgdorferi* in ear tissue. Significance determined by Student's *t* test for ankle swelling and Mann-Whitney *U* test for overall lesion. $^{**}p < 0.01$, $^{***}p < 0.001$.

Table I

Advanced congenics reveal impact of *Bbaa1* locus on infection-induced gene expression in CD45$^-$ cells from the joint tissue.

		ISRCL4 vs. B6		ISRCL3 vs. B6	
Gene	**Gene Title**[a]	**Fold Change**[b]	***p*-adj**[c]	**Fold Change**	***p*-adj**
Mstn	Myostatin	2.3	5.0E-16	2.4	2.8E-19
Nnt	Nicotinamide nucleotide transhydrogenase	1.7	1.6E-06	2.1	1.2E-14
Wdfy	WD repeat and FYVE domain containing 1	1.6	1.6E-12	1.8	1.5E-19
Gm21967	predicted gene, 21967	−1.9	3.9E-07	−2.5	9.6E-17
Ide	Insulin degrading enzyme	−1.6	1.6E-12	−1.9	1.6E-24

[a] Genes involved in *Bbaa1* Lyme arthritis development were independently identified in both ISRCL4 vs. B6 and ISRCL3 vs. B6 by RNA-seq 22 days post infection with *B. burgdorferi*.

[b] A positive value for fold change indicates gene expression was higher in CD45$^-$ cells isolated from congenic lines, negative fold change means expression was greater in CD45$^-$ cells harvested from B6 mice.

[c] Benjamini-Hochberg adjusted *p*-values from DESeq2